

Distribution of Aftershocks from Magnitude 7.8 Earthquake in Turkey

GEOL647
Salama Algaz
May 11, 2023

Introduction

Following a devastating earthquake of magnitude 7.8 in Turkey on February 06, 2023 many aftershocks ensued. The earthquake occurred at a depth of 10 km which is relatively shallow of an earthquake of such magnitude. Stronger earthquakes lead to more and stronger aftershocks. An earthquake occurs whenever the stress on rocks, caused by friction between tectonic plates, is released. The major earthquake carries most of the energy. However, some of the energy is transferred to nearby rocks along the fault line which then readjust themselves and cause the mini earthquakes (aftershocks) that follow large earthquakes (Rafferty, 2023). In this study I will be looking at the set of aftershocks that occurred around the vicinity of the major earthquake right after it happened and up to April 19, 2023 UTC 22:44:08. The end date was arbitrarily selected. Specifically I will be calculating the spread of the of the positions of the aftershocks. Figure 1 shows the positions of the aftershocks being studied.

The fact that the aftershocks occur along fault lines means that they can be observed to roughly map where these fault lines exist. From the image above there appears to be two main fault lines. As such the data is expected to have two directions in which there is significant spread. Additionally, I will attempt to model the dependence of the number of aftershocks on time (days) by using inversion theory. The model has the following form:

$$y = m_1 + \frac{m_2}{t^p}$$

where p is the order or decay rate. This can be written in matrix form as such $\begin{bmatrix} m_1 & m_2 \end{bmatrix} \begin{bmatrix} 1 \\ 1/t^p \end{bmatrix}$. Three values for p are tested: $p = 0.5, 1, 2$. For each model, I will minimize three objective functions, the L1, L2, and L_∞ norms, and compare the results with the data.

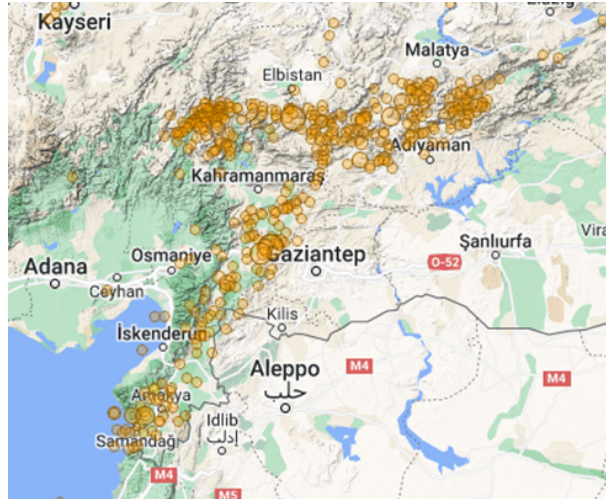


Figure 1: Image containing most of the aftershocks being studied. The sizes of the yellow dots indicate the magnitude. Image retrieved from https://ds.iris.edu/wilber3/find_event

Methods

The data downloaded from IRIS: Wilber 3 contained the date, latitude (deg), longitude (deg), depth (km), and magnitude of each aftershock. I chose the initial time ($t_0 = 0$) to be the event time of the 7.8 magnitude earthquake, which occurs at 02/06/2023 UTC 01:17:34. The time of each event is in reference to this date. To parse through the file I wrote a python code that reads the file and writes a new file containing the time (seconds), latitude (deg), longitude (deg), and depth (km). The reason for this is because it is easier to deal with dates in Python than in Matlab. I did not include the magnitudes as it is irrelevant to this study. See Appendix 2 for the Python code. The new file is then read by the Matlab script. The first section of the script computes the number of aftershocks each day. There are 73 days in the data file, so there are 73 frequencies for each day. The problem is considered linear and so is modeled by matrix multiplication: $G\mathbf{m} = d$, where \mathbf{m} is the vector containing the model parameters, G is the transformation matrix, and d is the data vector containing the number of aftershocks. The L1, L2, and L_∞ norms are defined in the script as follows:

$$\text{L1: } \sum |G\mathbf{m} - d|$$

$$\text{L2: } \sum (G\mathbf{m} - d)^2$$

$$L_\infty: \max(|G\mathbf{m} - d|)$$

With the objective functions defined, the function `fminsearch` is used to find the minimum of L1 and L_∞ . The minimum of the L2 norm is found using the function `linsolve` (which solves for $\hat{\mathbf{m}}$ in $G\hat{\mathbf{m}} = d$). The model parameters of each fit is displayed in the results section along with a plot containing the predicted frequencies from each fit and observed frequencies. This is done for $p = 0.5, 1, 2$.

The second section of the script analyzes the spread across the aftershocks, the covariance matrix of the positions of these aftershocks will be calculated. Before computing the covariance matrix the positions are converted to kilometers. One degree of latitude can be found by multiplying the radius of the Earth (6371 km) by $\pi/180$ which gives 111 km per degree of latitude. The average latitude at which the aftershocks occurs is 37 degrees. One degree of longitude at latitude 37 degrees is $6371 \cos(37^\circ) \approx 87\text{km}$. Once all the positions are in kilometers the mean is subtracted so that each position is centered around zero. The Eigenvalues and Eigenvectors of the covariance matrix is calculated. The eigenvalues give the amount of spread and the eigenvectors give the direction of spread. The directions of spread, scaled according to their magnitude of spread, is then plotted on top of the aftershocks along with a map.

Results

The relationship of the observed number of frequencies to number of days passed since the earthquake occurred can be glimpsed by plotting a histogram which is shown below in Figure 2. The data resembles exponential decay of the form: $N(t) = Ae^{-\alpha t}$ where N is the number of aftershocks, A is the number of aftershocks on the first day, and α is the decay rate. Such a function cannot be written directly in matrix form, however, if the logarithm is taken on both sides of the equation the result will yield $\ln(N(t)) = \ln(A) - \alpha t$ which can be written in matrix form:

$$\begin{bmatrix} \ln(A) & \alpha \end{bmatrix} \begin{bmatrix} 1 \\ -t \end{bmatrix}$$

Bearing in mind that the function would have to take in the logarithm of the data vector. Despite this modification, the Matlab function `linsolve` was not able to produce any model parameters, and so instead it was modeled with the equation: $N(t) = m_1 + m_2/t^p$, which resembles exponential decay.

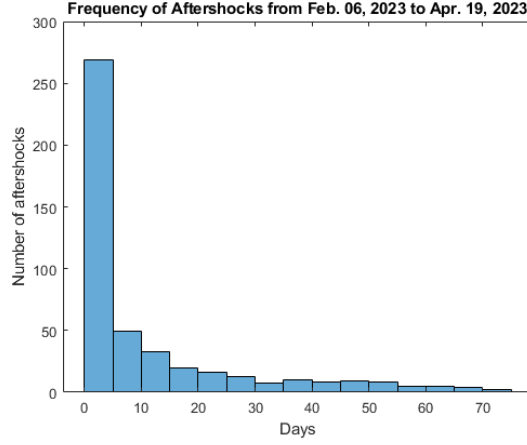


Figure 2: Histogram depicting the frequency of aftershocks

Table 1 shows the model parameters for each fit for $p = 1$, and Figure 3a shows the predicted frequencies along with the data. The L_∞ norm best predicts the frequency on the first day, but after day 9 it fails and in fact gives back negative numbers which are nonphysical. The predicted L_2 frequencies approximate the first couple of days, but after day 34 or 35 runs into the same issue as L_∞ does and gives back negative numbers. The L_∞ fit is not viable after day 9 and the L_2 fit is not viable after day 34, so both are short-term models. While the L_1 norm underestimates the frequency on the first couple of days, it best approximates later frequencies. The L_1 fit is capable of predicting frequencies for over a month.

Table 1: Model parameters for all p values for each norm fit going from top to bottom: L_1 to L_2 to L_∞ .

Fit	$m_1, p = 1$	$m_2, p = 1$	$m_1, p = 1/2$	$m_2, p = 1/2$	$m_1, p = 2$	$m_2, p = 2$
L_1	-0.8387	93.6775	-6.9462	56.4311	2.6286	163.1279
L_2	-3.2086	142.0094	-18.7866	116.6270	2.6286	161.1060
L_∞	-17.0882	162.1176	-58.2899	198.8896	6.7501	163.1697

Other values for p did not yield good results. As can be seen from Figure 3, the models with $p = 1/2$ and $p = 2$ are shifted away from the data in a systematic way. The $p = 1/2$ models *underestimate* the decay rate and so the predicted values sit below the observed data. On the other hand, the $p = 2$ models *overestimate* the decay rate and so the predicted values sit above the observed data. Most of the $p = 1/2$ models will have completely decayed by day 5, while the $p = 2$ models imply that aftershocks will never cease. This can be seen when you take the limit $t \rightarrow \infty$ of the equation: $N(t) = m_1 + m_2/t^p \rightarrow m_1$. For $p = 2$, all of the fits give positive m_1 , and so at large time scales there will still be aftershocks. Both of

these do not agree with observations. Therefore, the model function with $p = 1$ represents the most accurate depiction of the data.

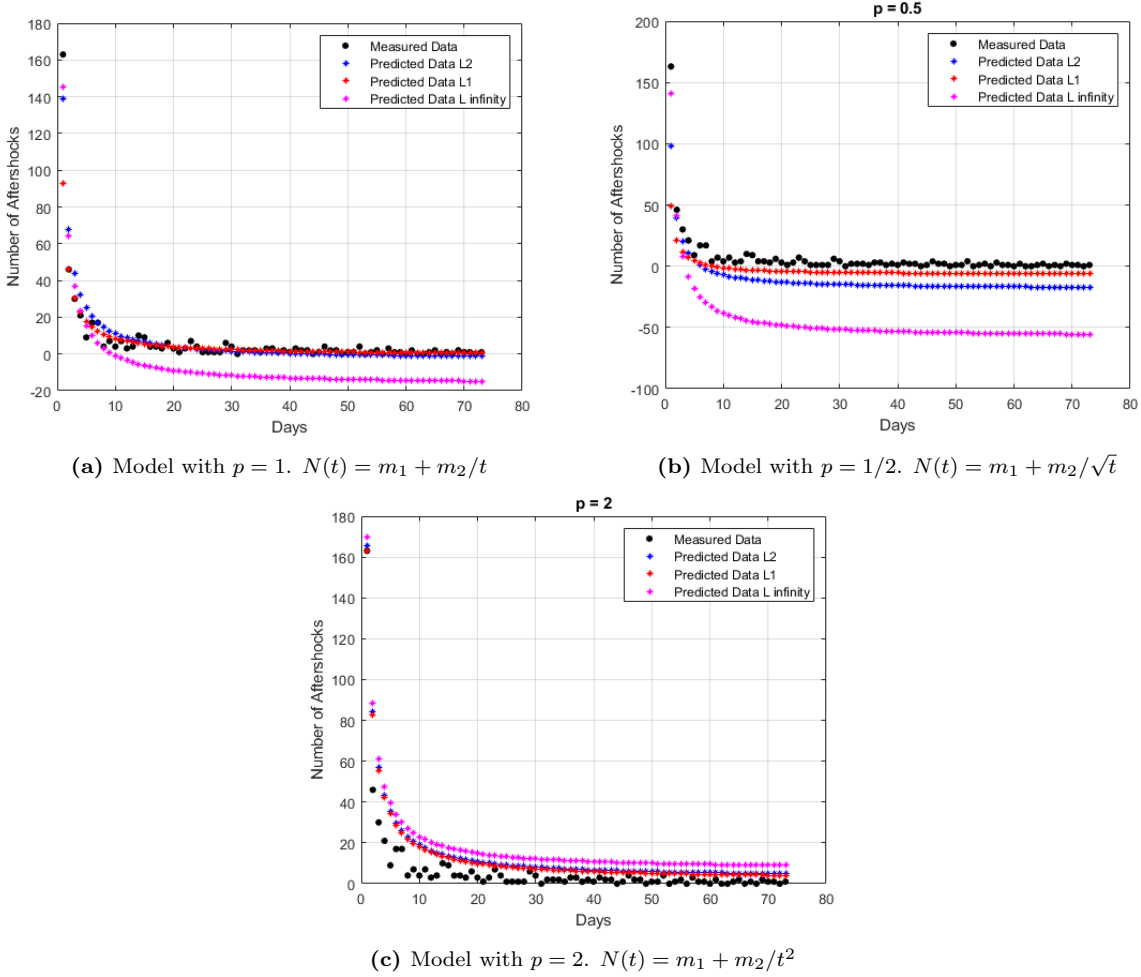


Figure 3: Best fit for 3 different values of p and 3 different objective functions for each value of p .

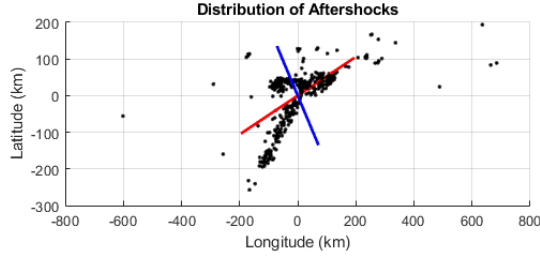
The second section of the results involves the variance of the positions of the aftershocks. Figure 4 shows the distribution in degrees and kilometers. The depiction of the spread on the z-axis has been omitted because it is relatively insignificant. It only spans 20 km at most which is much less than the spans of the other directions. The covariance matrix of the data is

$$C = \begin{bmatrix} 12,207 & 4,677 & 43 \\ 4,677 & 5,848 & -15 \\ 43 & -15 & 14 \end{bmatrix}$$

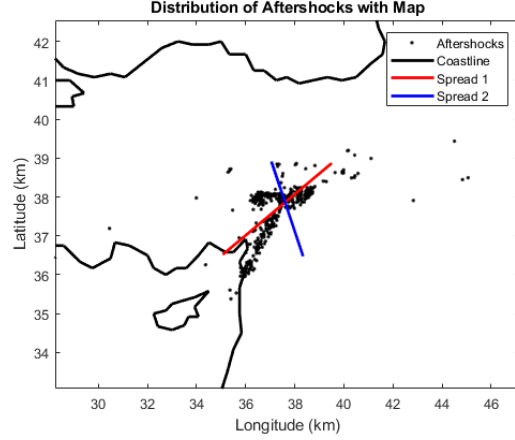
The values in the last row and column are small compared to the other values which is to be expected because the variance in z is very small. The eigenvalues of the matrix are given in Table 2. The largest eigenvalue is ten times bigger than the second largest. While it is not as large as the difference between λ_2 and λ_3 , it is not small. There is significant spread in two directions albeit more in one direction.

Table 2: Eigenvalues in decreasing order.

λ_1	λ_2	λ_3
14,683	3,373	13



(a) Positions of aftershocks in kilometers.



(b) Positions of aftershocks in degrees with reference to a map.

Figure 4: Visual distribution of aftershocks between Turkey and Syria. The colored lines are the eigenvectors which represent the direction of spread.

The eigenvectors of the matrix give the direction of spread. They are shown in Figure 4 as solid colored lines. The red line is the eigenvector corresponding to the eigenvalue λ_1 and the blue line corresponds to eigenvalue λ_2 (the last eigenvector has been omitted). The components of the eigenvectors are:

$$\mathbf{v}_1 = \begin{bmatrix} -0.8838 \\ -0.4679 \\ -0.0021 \end{bmatrix}, \mathbf{v}_2 = \begin{bmatrix} -0.4678 \\ -0.8838 \\ -0.0102 \end{bmatrix}, \mathbf{v}_3 = \begin{bmatrix} -0.0066 \\ -0.0080 \\ -0.9999 \end{bmatrix}$$

The standard deviation of the first direction of spread is 110 km, so 95% of the aftershocks fall within 220 km in longitude of the main earthquake. The standard deviation of the second spread is 76.5 km, so 95% of the aftershocks fall within 153 km in latitude. The standard deviation of the final spread is 3.7 km meaning the aftershocks are not deeper than about 15 km (recall that the depth is centered around zero so there is an extra factor of 2 to account for both up and down). These results seem to agree with Figure 4 and Figure 1. The 2 large eigenvalues also agree with the initial expectation of there being 2 directions of spread.

Conclusion

The number of aftershocks per day depends on how much time has passed since the earthquake. As more time passes, less aftershocks occur. Eventually, there are no more aftershocks. This motivated the question of how fast does the number of aftershocks decrease with time. At first it appeared to have the form of exponential decay, however, that didn't yield any parameters so an inverse law was fitted. The model that best fit the data had order $p = 1$. Having found a satisfactory model equation, I searched for resources where an equation relating frequency of aftershock to time was derived. Interestingly, I found Omori's paper "On the Aftershocks of Earthquakes" where he similarly tried to fit an exponential decay as I have and having found it unsatisfactory he fit it to this equation: $y = \frac{k}{h+t}$, which is called Omori's law (1894). It has the same time dependence as the equation fitted in this paper, namely that $y \propto 1/t$, however the choice of parameters is slightly different. Utsu extends Omori's law to $y = k/(h+t)^p$ where p usually has values between $0.7 < p < 1.5$. This agrees with the findings of the paper that outside these limits the model fails. It would be interesting to fit the data to Omori's law, compare it to the fit in this paper and observe which fit is more ideal (this was not done in this study as Omori's law couldn't be modeled with matrix multiplication). Moreover, the two equations can be fitted to other sets of aftershocks thus increasing the sample size which would lead to a more confident conclusion. Another extension would be to do fits for p values between the limits that were set in this paper (i.e. $0.5 < p < 2$) or between the limits set by Utsu (i.e. $0.7 < p < 1.5$). The analysis on the covariance matrix of the distribution of aftershocks revealed two major directions in which spread is significant. This agrees with expectations. Although, other distributions of aftershocks usually show 1 direction of spread which is in the same direction as the fault line. In this case, the 2 directions of spread indicate 2 fault lines. This shows that the earthquake occurred around the critical point at which the Arabian, African, and Eurasian tectonic plates meet. A more in-depth analysis would be to find the positions of the fault lines.

References

- [1] Class Lectures
- [2] Data is retrieved from https://ds.iris.edu/wilber3/find_event
- [3] Omori, F. (1894) On the Aftershocks of Earthquakes. Journal of the College of Science, Imperial University of Tokyo, 7, 111-120.
- [4] Rafferty, J. P. (2023, May 5). Aftershock. Encyclopædia Britannica.
- [5] Utsu, T. (1961). "A statistical study of the occurrence of aftershocks". Geophysical Magazine. 30: 521–605.